Analysis of Runx1 Using Induced Gene Ablation Reveals Its Essential Role in Pre-liver HSC Development and Limitations of an In Vivo Approach

Stem Cell Reports
Article

ISSCR

OPEN ACCESS

Analysis of *Runx1* Using Induced Gene Ablation Reveals Its Essential Role in Pre-liver HSC Development and Limitations of an *In Vivo* Approach

Jordi Senserrich,[1,3] Antoniana Batsivari,[1] Stanislav Rybtsov,[1] Sabrina Gordon-Keylock,[1] Celine Souilhol,[1,4] Frank Buchholz,[2] David Hills,[1] Suling Zhao,[1] and Alexander Medvinsky[1,*]

[1]MRC Centre for Regenerative Medicine, University of Edinburgh, Edinburgh EH16 4UU, UK
[2]Max Planck Institute of Molecular Cell Biology and Genetics, Technische Universität Dresden, Dresden 01307, Germany
[3]Present address: Institut d'Investigació Biomèdica de Bellvitge (IDIBELL), Barcelona 08908, Spain
[4]Present address: Department of Infection, Immunity & Cardiovascular Disease, University of Sheffield, Sheffield S10 2RX, UK
*Correspondence: a.medvinsky@ed.ac.uk
https://doi.org/10.1016/j.stemcr.2018.08.004

SUMMARY

Hematopoietic stem cells (HSCs) develop in the embryonic aorta-gonad-mesonephros (AGM) region and subsequently relocate to fetal liver. *Runx1* transcription factor is essential for HSC development, but is largely dispensable for adult HSCs. Here, we studied tamoxifen-inducible *Runx1* inactivation *in vivo*. Induction at pre-liver stages (up to embryonic day 10.5) reduced erythromyeloid progenitor numbers, but surprisingly did not block the appearance of *Runx1*-null HSCs in liver. By contrast, *ex vivo* analysis showed an absolute *Runx1* dependency of HSC development in the AGM region. We found that, contrary to current beliefs, significant Cre-inducing tamoxifen activity persists in mouse blood for at least 72 hr after injection. This deferred recombination can hit healthy HSCs, which escaped early *Runx1* ablation and result in appearance of *Runx1*-null HSCs in liver. Such extended recombination activity *in vivo* is a potential source of misinterpretation, particularly in analysis of dynamic developmental processes during embryogenesis.

INTRODUCTION

In the mouse, the first transient hematopoietic waves (primitive erythroid and erythromyeloid progenitors [EMPs]) emerge extra-embryonically in the early yolk (McGrath et al., 2015; Palis et al., 1999). HSCs, which give rise to the adult hematopoietic system, appear only by mid-gestation intra-embryonically within the aorta-gonad-mesonephros (AGM) region (Ciau-Uitz et al., 2016; Medvinsky and Dzierzak, 1996; Medvinsky et al., 1993; Muller et al., 1994). HSCs emerge predominantly from the endothelial floor of the dorsal aorta (de Bruijn et al., 2002; North et al., 2002; Taoudi and Medvinsky, 2007) through a maturation process defined by inductive interactions within the AGM region (Fitch et al., 2012; Souilhol et al., 2016a) and signals from somites (Clements et al., 2011; Lee et al., 2014; Pouget et al., 2014). The origin of HSCs from aortic endothelium is supported by strong evidence in non-mammalian vertebrates and in humans (Bertrand et al., 2010; Ivanovs et al., 2014; Kissa and Herbomel, 2010).

Various signaling pathways are involved in early hematopoietic development (reviewed in [Ciau-Uitz et al., 2016]). HSC maturation in the mouse is a multistep process driven by SCF and IL3 (Robin et al., 2006; Rybtsov et al., 2011, 2014), accompanied by temporal changing signaling requirements for *Notch*, *Shh*, and *Bmp* (Gama-Norton et al., 2015; Lizama et al., 2015; Peeters et al., 2009; Richard et al., 2013; Souilhol et al., 2016a, 2016b). It is reasonable to assume that exact transcription factor machinery also attunes. Here we aimed to explore temporal requirements for *Runx1*, a transcription factor essential for HSC development, but which is far less significant in adult bone marrow HSCs (Cai et al., 2011; North et al., 1999; Okuda et al., 1996; Putz et al., 2006). EMPs and HSCs originate from different endothelial subsets through a *Runx1*-dependent process (Chen et al., 2011; Eliades et al., 2016; Lie et al., 2018). Conditional *Runx1* ablation *in vivo* blocks the endothelial to EMP/HSC transition prior to liver colonization (Chen et al., 2009). More detailed analysis using a robust AGM explant system recapitulating HSC development, showed that, up to embryonic day 11.5 (E11.5) (immediately prior to fetal liver colonization), HSC development absolutely depends on *Runx1*, but EMPs become *Runx1* independent at earlier stages (Tober et al., 2013).

Here we followed the consequences of induced *Runx1* ablation in the AGM region on HSC development in the fetal liver. We used a tamoxifen (4-OHT)-inducible Cre-ERT2 system to delete *Runx1* and assessed the presence of EMPs and definitive HSCs in the E13.5 fetal liver. We observed a significant reduction of EMP numbers, but, contrary to our expectations and in apparent discrepancy with a previous report (Tober et al., 2013), we detected significant numbers of *Runx1*-null HSCs in the liver, implying that HSC development in the AGM region does not require *Runx1*. We then performed *in vivo* injections of 4-OHT, but in this case isolated E11.5 AGM regions and after culture transplanted them into irradiated recipients. We found no *Runx1*-null HSCs in repopulated irradiated recipients, which is in conflict with results of *in vivo* analysis.

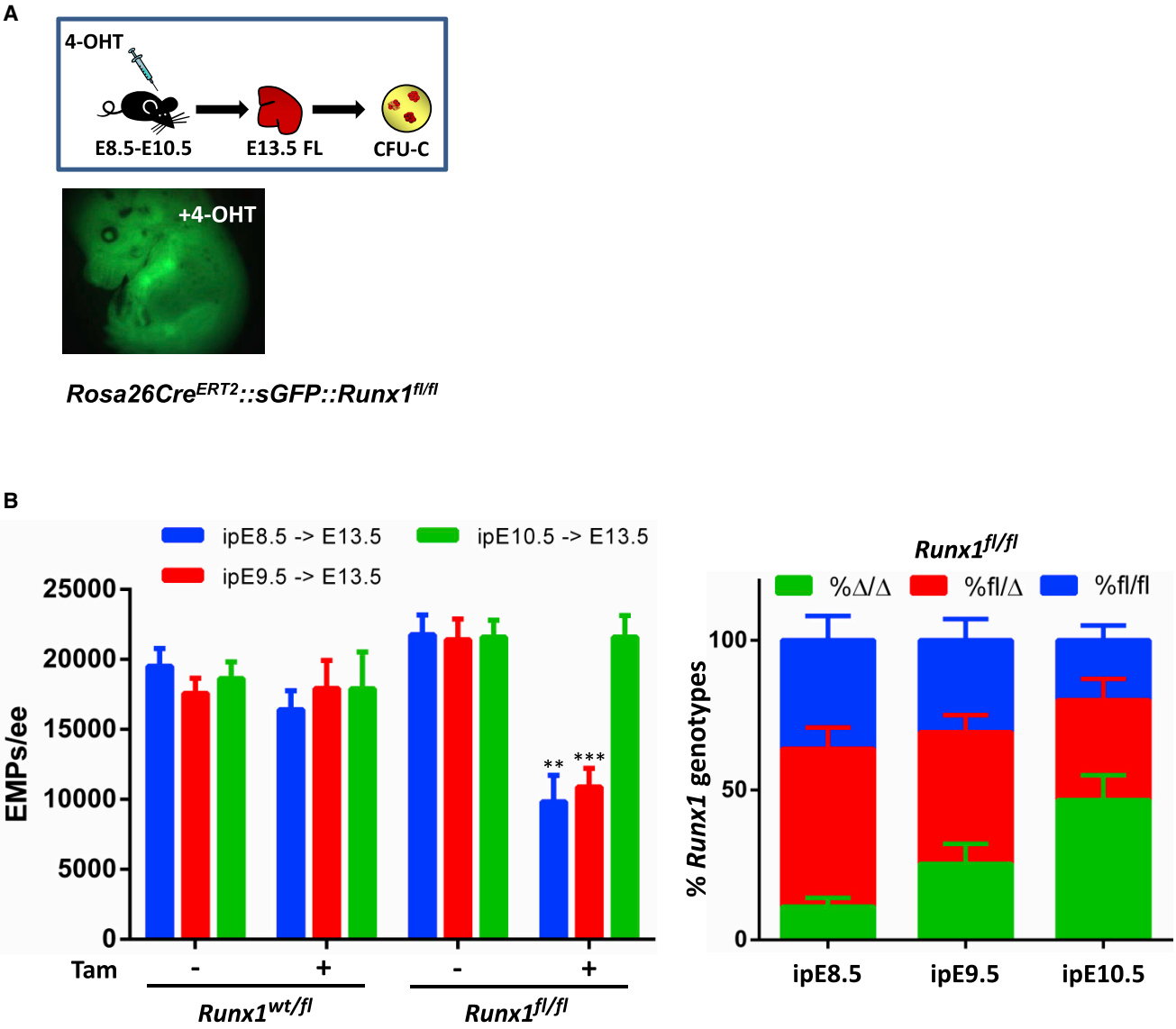

(legend on next page)

In search of an explanation, we tested how long 4-OHT or/and its active derivatives (cumulatively termed here 4-OHT/Der) remain in the circulation of adult mouse and found that, at least 3 days after injection, concentration of 4-OHT/Der in the peripheral blood of the animal remains sufficient to cause significant (up to 20%) Cre-mediated recombination in cells. Therefore, those HSCs, which have not recombined during the AGM stage could proceed with development, but could be hit by recombination later when *Runx1* is no longer essential. This would inevitably lead to emergence of functionally active *Runx1*-null HSCs in the fetal liver. Such a problem does not exist when the AGM region is removed from the mouse and explanted in fresh culture medium free of 4-OHT/Der.

Thus, despite the advantages of *in vivo* analysis in principle, poor control over *in utero* development may bring about a significant uncertainty and cause misinterpretation of results. By contrast, the functionally validated and robustly controlled *ex vivo* system provides strong evidence for the essential role of *Runx1* in HSC development, in keeping with previously published results.

RESULTS

4-OHT-Induced *Runx1* Ablation at E8.5–E9.5, but Not Thereafter, Reduces EMP Formation

Here, we studied effects of *in-vivo*-induced stage-specific *Runx1* ablation on the appearance of EMPs in fetal liver. To this end, pregnant [$Rosa26Cre^{ERT2}$:*sGFP*:$Runx1^{fl/fl}$] females crossed with [$Rosa26Cre^{ERT2}$::*sGFP*::$Runx1^{wt/fl}$] males were treated with a single dose of 4-OHT between 8.5 and 10.5 days of gestation at a concentration of 2 mg/mouse. E13.5 litters containing both homozygous $Runx1^{fl/fl}$ and heterozygous $Runx1^{wt/fl}$ (control) embryos were harvested, and cell suspensions prepared from individual livers were analyzed in methylcellulose colony-forming unit (CFU) assays (Figure 1A). In homozygous $Runx1^{fl/fl}$ embryos ([$Rosa26Cre^{ERT2}$::*sGFP*::$Runx1^{fl/fl}$]), 4-OHT injections at E8.5 or E9.5 led to a significant reduction of fetal liver EMPs by ~50% compared with $Runx1^{wt/fl}$ heterozygous [$Rosa26Cre^{ERT2}$::*sGFP*::$Runx1^{wt/fl}$] controls (Figure 1B, blue and red bars). However, 4-OHT injection at later stage (E10.5) had no effect on EMPs in fetal livers (Figure 1B, green bars), indicating the essential role of *Runx1* in EMP development at early stages but not after E10.5. This result is in agreement with temporal Runx1 dependency in embryonic EMPs reported previously (Tober et al., 2013).

To confirm this conclusion, we tested the status of *Runx1* loci in individual fetal liver EMPs using PCR. We picked only liver-derived methylcellulose colonies expressing GFP, indicative of prior activity of Cre-recombinase. Due to their clonal origin, PCR analysis of individual CFU colonies reveals the *Runx1* status of individual EMPs. We found that a fraction of tested colonies (20%–36%) escaped any *Runx1* recombination despite activation of GFP (Figures 1B right, 1C, and S1A; Table 1). The recombined fraction (64%–80%) contained those colonies that retained one intact *Runx1* allele ($Runx1^{fl/\Delta}$) or had both loci recombined ($Runx1^{\Delta/\Delta}$). Of note, 4-OHT injection at E8.5, E9.5, and E10.5 resulted in progressive growth of the proportion of $Runx1^{\Delta/\Delta}$ EMPs in the FL (11%, 25%, and 47%, respectively) (Figures 1B right and 1C; Table 1). A particularly high fraction of $Runx1^{\Delta/\Delta}$ EMPs was observed after 4-OHT injection at E10.5, when no reduction of EMP numbers was observed. All together this implies progressive acquisition of *Runx1* independency by EMPs during development, in line with a previous report (Tober et al., 2013).

Induced *Runx1* Ablation from E9.5 onward Does Not Eliminate HSC Development in the Fetal Liver

We tested whether a single 4-OHT injection between E8.5 and E10.5 would block HSC development *in vivo*. After injection, embryos continued development *in utero* until E13.5. Cells from individual E13.5 fetal livers were then isolated and transplanted separately into irradiated recipients, as depicted in (Figure 2A). To our surprise, robust multilineage donor-derived long-term engraftment was observed in all 37 recipient animals, regardless of injection time (Figure 2B, left, and data not shown). Cre activity in these experiments was very efficient as seen by the presence of a large GFP+ cell fraction in most recipients (ranging from 85% to 97%, Figure S2).

Figure 1. Tamoxifen (4-OHT)-Induced *Runx1* Ablation at E8.5–E9.5, but Not Thereafter, Reduces EMP Formation

(A) Experimental design: studying the effect of conditional *Runx1* deletion on EMPs. A single dose of 4-OHT was administered intraperitoneally (i.p.) to [$Rosa26Cre^{ERT2}$::*sGFP*::$Runx1^{fl/fl}$] pregnant females crossed with [$Rosa26Cre^{ERT2}$::*sGFP*::$Runx1^{wt/fl}$] males at E8.5–E10.5. E13.5 embryos were collected and EMPs from individual FLs quantified by clonogenic methylcellulose assays. A representative 4-OHT-induced E13.5 GFP+ embryo is shown.

(B) Left: numbers of E13.5 FL EMPs per embryo equivalent (e.e.). Time of i.p. injection indicated for, e.g., as ipE8.5. Mean values and standard errors are shown (three independent experiments, at least three embryos in each experiment). Unpaired Student t statistical tests were performed (**p = 0.001; ***p = 0.0002). Right: *Runx1* recombination in [$Rosa26Cre^{ERT2}$::*sGFP*::$Runx1^{fl/fl}$] E13.5 FL erythromyeloid progenitors after 4-OHT injection at pre-liver stages, indicating the percentage of each genotype (at least two independent experiments; mean values and standard errors shown).

(C) Representative *Runx1* genotyping PCR gels of EMP colonies, showing wt, fl, and Δ bands.

Table 1. *Runx1* Status of E13.5 Fetal Liver GFP+ Erythromyeloid Progenitors (CFU-Cs) Derived from Individual Embryos after 4-OHT Injection at Pre-liver Stages

Experiment	Embryo Genotype	Embryos with *Runx1* Recombined Alleles/Total Embryos (Recombination Range) CFU-Cs in E13.5 FL			Total Colonies Analyzed
		wt/Δ	fl/Δ	Δ/Δ	
iE8.5 -> E13.5 FL	*R26CreERT2::Runx1*$^{wt/fl}$	9/9 (11%–42%)			111
	R26CreERT2::Runx1$^{fl/fl}$		12/13 (17–86%)	9/13 (6%–33%)	159
iE9.5 -> E13.5 FL	*R26CreERT2::Runx1*$^{wt/fl}$	7/7 (8%–58%)			85
	R26CreERT2::Runx1$^{fl/fl}$		13/13 (14%–80%)	11/13 (8%–67%)	134
iE10.5 -> E13.5 FL	*R26CreERT2::Runx1*$^{wt/fl}$	5/6 (33%–100%)			36
	R26CreERT2::Runx1$^{fl/fl}$		10/12 (20%–80%)	11/12 (20%–100%)	60

Recombination range refers to proportion of recombined colonies.

Since Cre-mediated GFP activation does not guarantee *Runx1* recombination in the same cells, the recombination status of *Runx1* was verified using PCR. To this end, individual donor-derived GFP+ colonies obtained from blood and bone marrow of long-term (16 weeks) reconstituted animals were analyzed by PCR (Figures 2B right, 2C, and S1B; Table 2). When 4-OHT was injected at E8.5, all but one GFP+ donor-derived methylcellulose colonies obtained cumulatively from 18 recipients contained at least one functional *Runx1* allele, indicating that *Runx1*$^{\Delta/\Delta}$ HSCs did not develop. However, injection at E9.5 gave a significant proportion of donor-derived *Runx1*$^{\Delta/\Delta}$ colonies (17%) in 13 repopulated recipients. Injection at E10.5 resulted in further increase (33%) of *Runx1*$^{\Delta/\Delta}$ donor-derived colonies obtained from long-term transplanted animals (a total of six recipients were analyzed) (Figures 2B right and 2C; Table 2).

Taken alone, these results suggest that *Runx1* is not required for HSC development from as early as E9.5, which contradicts the previous report showing *Runx1* dependency of HSC development up to E11.5 (Tober et al., 2013). We investigated reasons for this discrepancy as described below.

Active Concentrations of 4-OHT or/and Its Derivatives Persist in the Mouse for No Less than 72 hr

We reasoned that if, after 4-OHT injection, recombination does not occur in all cells at once and 4-OHT activity continues further, HSCs (known to become *Runx1* independent when fully mature) may undergo late *Runx1* ablation without adverse consequences. Upon transplantation, such *Runx1*-null HSCs could be generating *Runx1*$^{\Delta/\Delta}$ progeny detectable in the methylcellulose assay.

To investigate this possibility, we tested how long 4-OHT/Der persists in the mouse and causes recombination. To this end, wild-type C57BL/6 adult females were intraperitoneally injected with 4-OHT, and serum obtained at different time points after injection was added to cultures of primary AGM cells isolated from E10.5 and E11.5 [*RosaCreERT2::sGFP*] embryos (Gilchrist et al., 2003) (Figure 3A). We observed maximum recombination efficiency (100% GFP activation) using serum obtained 5 hr after 4-OHT administration. Nevertheless, serum collected after 48 and 72 hr could also cause 20%–40% recombination (Figure 3B). Specifically, 72 hr serum caused 52% ± 8.7% recombination in CD45+ cells, 16% ± 7.6% in VE-Cad+ cells, and 26% ± 13.2% in stromal cells (CD45−VE-Cad–) (data not shown). (Note that recombination in non-hematopoietic cells is underestimated due to known mosaicism of GFP expression in non-hematopoietic cells in these mice [Gilchrist et al., 2003]).

These experiments show that, after injection of 4-OHT, cells in the mouse containing *loxP* sites can recombine over a period of at least 3 days. Thus, those cells in the embryo which have not undergone rapid Cre-mediated recombination of the *Runx1*^{flox} allele continue to be exposed to 4-OHT/Der and can recombine, even 3 days after 4-OHT injection.

The extended circulation of 4-OHT/Der *in vivo* creates uncertainty as to when exactly during development *Runx1* becomes dispensable for HSC development. The next set of experiments was designed to control and reduce the duration of HSC exposure to 4-OHT/Der to obtain more interpretable results.

Runx1 Deletion at E9.5 Abrogates HSC Activity in the E11.5 AGM Region

To avoid prolonged exposure to 4-OHT/Der, we switched from the entirely *in vivo* design to experiments incorporating a highly controllable *in vitro* HSC maturation system (Rybtsov et al., 2011, 2014; Taoudi et al., 2008). As in previous setups, embryos for these experiments contained either

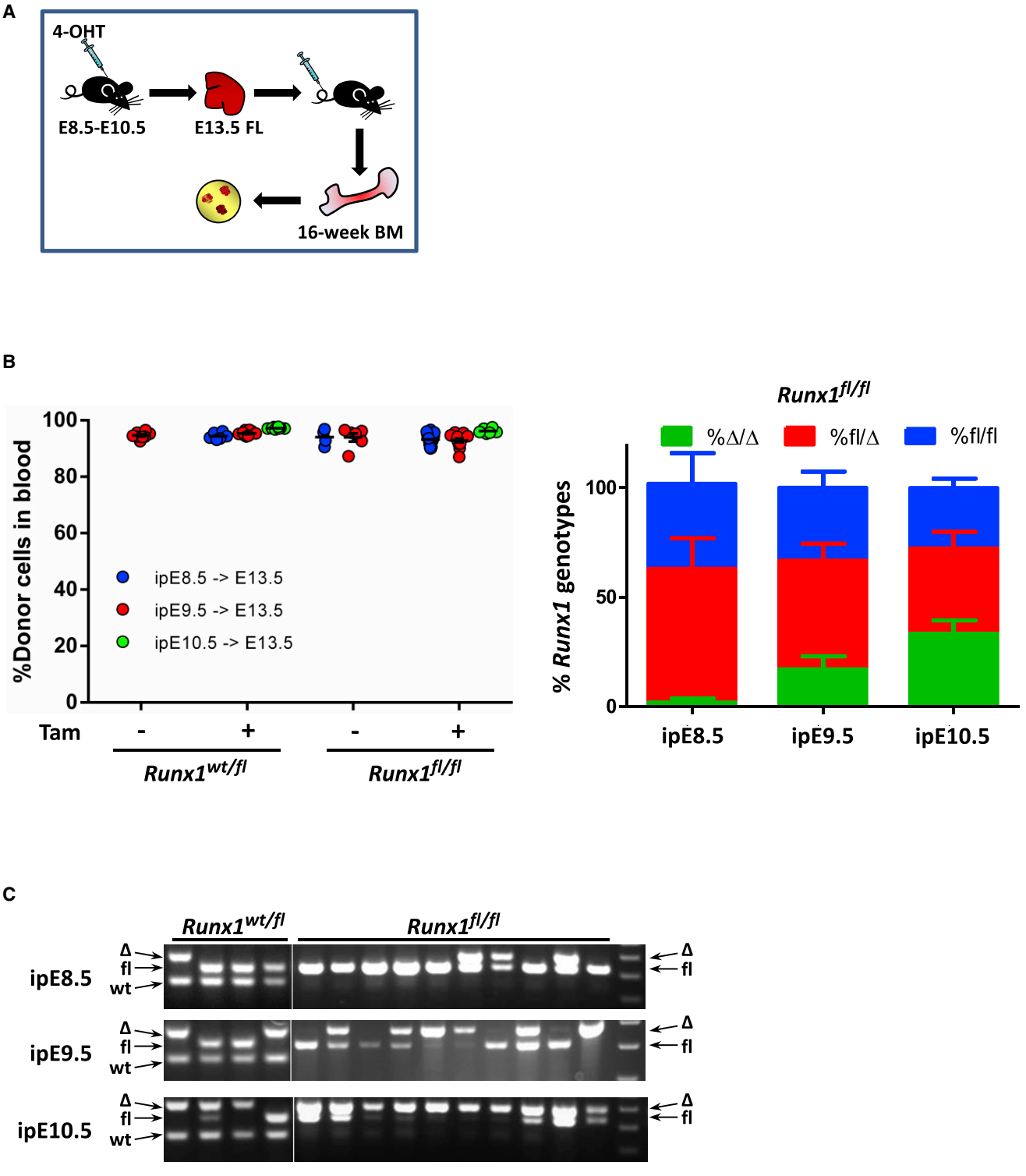

Figure 2. Induced *Runx1* Ablation from E9.5 onward Does not Eliminate HSC Development in the Fetal Liver

(A) Experimental design analogous to that described in Figure 1A, with cell suspensions from individual E13.5 FL embryos transplanted into irradiated adult mice.

(B) Left: donor-derived contribution in recipient mice blood 16 weeks after transplantation is shown. Each point represents an individual recipient mouse, representing data from at least two independent experiments. Numbers of analyzed mice for $Runx1^{wt/fl}$+ 4-OH-T series

(legend continued on next page)

Table 2. *Runx1* Status of E13.5 Fetal Liver HSCs Assessed by PCR Analysis of Donor-Derived GFP+ Erythromyeloid Progenitors from Long-Term Engrafted Recipients

		Embryos with *Runx1* Recombined Alleles/Total Embryos (Recombination Range)			Total Colonies Analyzed
		HSC-Derived CFU-Cs (BM + Blood)			
Experiment	Embryo Genotype	wt/Δ	fl/Δ	Δ/Δ	
iE8.5 -> E13.5 FL	*R26CreERT2::Runx1*$^{wt/fl}$	3/7 (17%–50%)			33
	R26CreERT2::Runx1$^{fl/fl}$		8/11 (33%–100%)	1/11 (8%)	89
iE9.5 -> E13.5 FL	*R26CreERT2::Runx1*$^{wt/fl}$	5/5 (6%–55%)			63
	R26CreERT2::Runx1$^{fl/fl}$		8/8 (18%–80%)	5/8 (10%–40%)	143
iE10.5 -> E13.5 FL	*R26CreERT2::Runx1*$^{wt/fl}$	2/3 (71%–100%)			9
	R26CreERT2::Runx1$^{fl/fl}$		3/3 (31%–54%)	3/3 (23%–44%)	52

Recombination range refers to proportion of recombined colonies.

both or one conditional *Runx1* allele (*Runx1*$^{fl/fl}$ and *Runx1*$^{wt/fl}$, respectively). 4-OHT was administered *in vivo* at E9.5 as described previously; but, instead of allowing the embryos develop *in utero* until E13.5, E11.5 AGM regions were dissected and individually explanted (Medvinsky and Dzierzak, 1996). Placement of the AGM region in fresh culture medium ends the exposure of developing HSCs to 4-OHT/Der. After 4 days in culture, AGM cells were transplanted into irradiated recipients (Figure 4A).

Twelve recipients transplanted with control [*Rosa26Cre*^{ERT2}*::sGFP::Runx1*$^{wt/fl}$] AGM cells showed high-level, long-term multilineage donor-derived engraftment. Fourteen of 16 recipients transplanted with [*Rosa26Cre*^{ERT2}*:: sGFP::Runx1*$^{fl/fl}$] AGM cells were also repopulated at high level (only one showed low-level donor-derived chimerism and one lacked engraftment) (Figure 4B). We observed highly efficient GFP recombination in [*Rosa26Cre*^{ERT2}*::sGFP::Runx1*$^{wt/fl}$] and [*Rosa26 Cre*^{ERT2}*::sGFP::Runx1*$^{fl/fl}$] repopulated cells (98% and 89%, respectively) (Figure S3). However, analysis of methylcellulose colonies obtained from these 14 long-term repopulated mice showed that, by contrast to liver, [*Rosa26Cre*^{ERT2}*:: sGFP::Runx1*$^{fl/fl}$] AGM region transplants contained no *Runx1*$^{\Delta/\Delta}$ HSCs (repopulated mice gave no *Runx1*$^{\Delta/\Delta}$ myeloid colonies) (Figure 4C; Table 3), indicating an absolute requirement of *Runx1* for HSC development prior to liver colonization. Of note, variance in efficiency of recombination suggests a considerable difference in accessibility of *loxP* sites for Cre-mediated recombination between GFP and *Runx1* loci.

DISCUSSION

During maturation, pre-HSCs undergo massive expansion in the AGM region, sequentially upregulating hematopoietic CD41, CD43, and CD45, and some other markers (Boisset et al., 2015; Ferkowicz et al., 2003; Rybtsov et al., 2011, 2014, 2016; Taoudi et al., 2008; Tober et al., 2018; Zhou et al., 2016). This stepwise developmental process is driven by dynamic gene actions. Temporal requirements for genes driving HSC development can vary, and accurate staging of gene involvement is essential for understanding this process. For example, acquisition of adult phenotype is accompanied by gradual loss of *Notch*, *Shh*, and *Bmp* dependency by HSCs in the AGM region (Gama-Norton et al., 2015; Lizama et al., 2015; Peeters et al., 2009; Richard et al., 2013; Souilhol et al., 2016a, 2016b).

Runx1 is a key transcription factor involved in EMP and HSC development (Cai et al., 2000; Chen et al., 2009; North et al., 2002; Okuda et al., 1996). However, exact action points of *Runx1* during this multistep process require clarification. Initial hematopoietic specification associated with upregulation of CD41 does not require *Runx1* (Liakhovitskaia et al., 2014). *Runx1* sensitivity of the embryonic endothelium is limited to the period around E7.5–E8.5 (Tanaka et al., 2012; Yzaguirre et al., 2018). Induced stage-specific inactivation using explant cultures followed by long-term transplantations showed that, up to E11.5, Runx1 is absolutely required for HSC development but becomes dispensable after that (Tober et al., 2013). Here we

(ipE8.5, ipE9.5, and ipE10.5) were 6, 10, and 10, respectively; for *Runx1*$^{fl/fl}$+ 4-OH-T series (ipE8.5, ipE9.5, and ipE10.5) were 18, 13, and 6, respectively. Right: *Runx1* status of [*Rosa26Cre*^{ERT2}*::sGFP::Runx1*$^{fl/fl}$] E13.5 FL HSCs, assessed by analysis of donor-derived erythromyeloid progenitors from long-term (16 weeks) engrafted recipients. Percentages of each genotype (at least two independent experiments; mean values and standard errors) are shown.

(C) Representative *Runx1* genotyping PCR gels of HSC-derived progenitors, indicating wt, fl, and Δ bands, are shown.

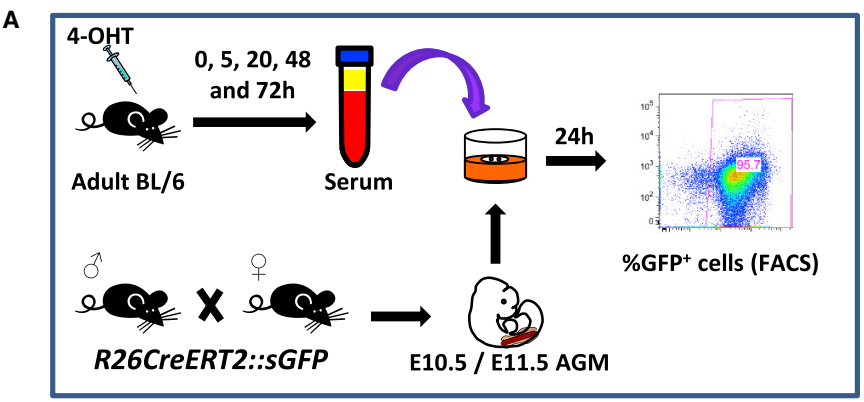

Figure 3. Active Concentrations of 4-OHT or/and Its Derivatives Remain in the Mouse for No Less than 72 hr

(A) Experimental schematics: wild-type C57BL/6 adult females were intraperitoneally injected with 4-OHT and serum obtained at different time points after injection. Then, it was added to cultures of primary E10.5 and E11.5 [*RosaCreERT2::sGFP*] AGM cells, and recombination was assessed by monitoring GFP expression by fluorescence-activated cell sorting after 24 hr.

(B) GFP recombination in AGM cells upon incubation with serum isolated at different time points (0, 5, 20, 48, and 72 hr) after 4-OH-tamoxifen intraperitoneal injection (at least two independent experiments; three mice/experiment; mean values and standard errors are shown).

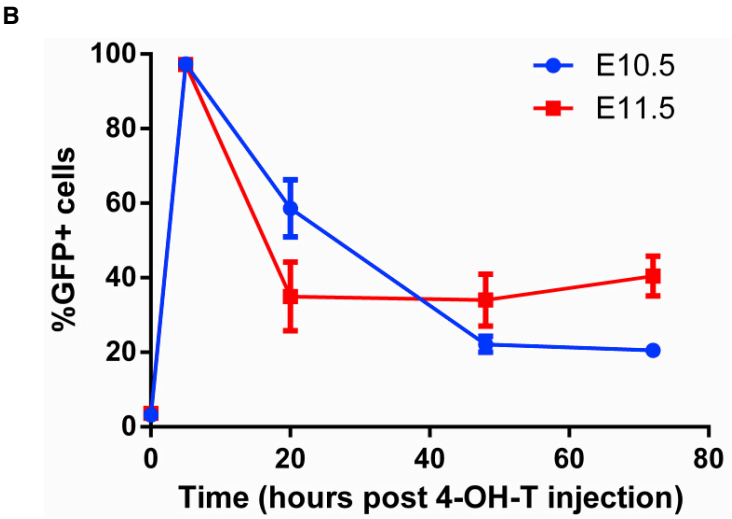

explored whether the conclusions of this study can be corroborated by *in vivo* tracking.

To this end, we injected pregnant females with 4-OHT during active EMP/HSC formation. Instead of analysis of E11.5 AGM explants (Tober et al., 2013), we followed HSC development *in utero* up to E13.5 in the fetal liver. Injections at E8.5/E9.5, but not at E10.5, reduced EMP numbers in the E13.5 liver, indicating that by this stage EMPs become *Runx1* independent, which was corroborated by increased emergence of $Runx1^{\Delta/\Delta}$, in agreement with previously reported results (Tober et al., 2013).

We then focused on the HSC development. After a single 4-OHT injection at E8.5, E9.5, or E10.5, the embryos were allowed to develop *in utero* up to E13.5, after which fetal liver cells were transplanted into irradiated recipients. Unexpectedly, all long-term repopulated animals (transplanted with E9.5 cells onward) contained *Runx1*-null HSCs, in apparent contradiction with previous data obtained in AGM cultures (Tober et al., 2013).

We then reasoned that *in vivo* results might depend on the persistence of 4-OHT/Der activity in the mouse. Indeed, 4-OHT injections at E8.5/E9.5 yielded non-recombined ($Runx1^{fl/fl}$) and partly recombined ($Runx1^{fl/\Delta}$) HSCs. If 4-OHT/Der persisted in the mouse beyond E11.5 stage (when HSCs become *Runx1* independent), delayed recombination could transform non-recombined ($Runx1^{fl/fl}$) and partly recombined ($Runx1^{fl/\Delta}$) HSCs into $Runx1^{\Delta/\Delta}$ HSCs without adverse effect. Indeed, we found that substantial 4-OHT/Der activity, capable of inducing CRE-ERT2, persists in the mouse for at least 3 days, introducing major uncertainty as to when exactly recombination took place and making *in vivo* experiments poorly interpretable. Crucially, under highly controlled experimental conditions, where after a single 4-OHT injection at E9.5, E11.5 AGM regions

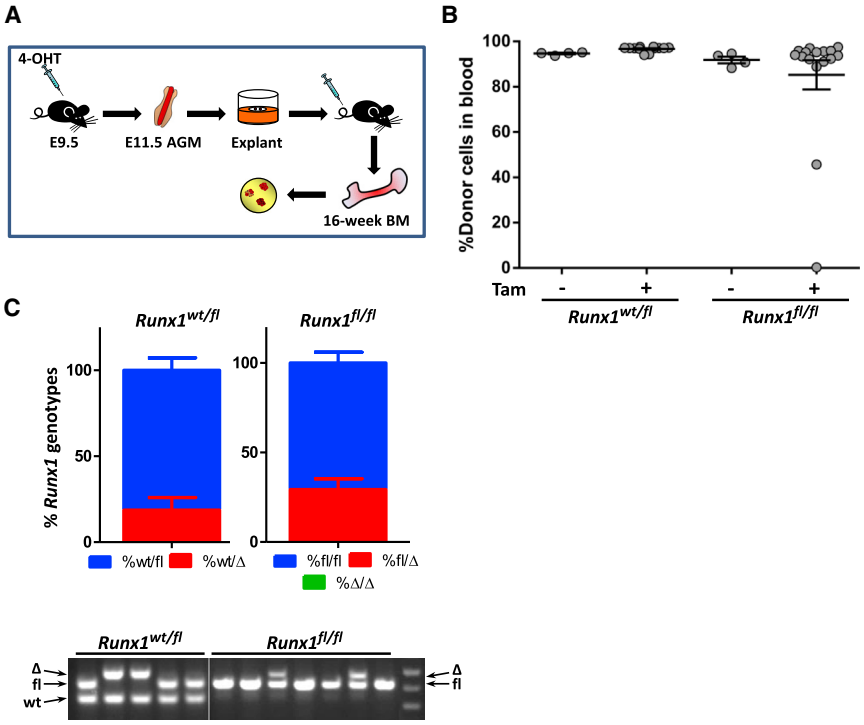

Figure 4. *Runx1* Deletion at E9.5 Abrogates HSC Activity in the E11.5 AGM Region

(A) 4-OHT-induced *Runx1* deletion was performed at E9.5 as described in Figure 1A, but embryos were harvested at E11.5. AGM regions were dissected and cultured as explants for 4 days, and cell suspensions from individual explants were transplanted into irradiated adult mice.

(B) Donor-derived engraftment in the blood from recipient mice 16 weeks after transplantation is shown. Each point represents an individual recipient mouse (data from three independent experiments). Numbers of analyzed mice for $Runx1^{wt/fl}$ and $Runx1^{fl/fl}$+ 4-OH-T conditions were 12 and 16, respectively.

(C) Top: recipient mice were sacrificed 16 weeks after transplantation and the *Runx1* genotype was examined by PCR in individual donor-derived GFP+ CFU-Cs from bone marrow and blood. *Runx1* genotype frequencies within donor-engrafted mice are plotted. Average and SE from embryos from three independent experiments are given (no production of $Runx1^{\Delta/\Delta}$ colonies observed). Bottom: representative *Runx1* genotyping PCR gels of colonies, with *Runx1* wt, fl, and Δ bands shown.

were isolated and cultured in fresh medium free of 4-OHT/Der, subsequent transplantations showed complete ablation of *Runx1*-null HSCs. This result points to a critical role for *Runx1* in HSC development in the AGM region before colonization of the fetal liver, in agreement with a previous report (Tober et al., 2013).

Interestingly, although we observed near 100% recombination of the GFP transgene, the efficiency of *Runx1* recombination was significantly lower, emphasizing that accessibility of *loxP* sites in various genetic loci further confounds interpretation of *in vivo* results. Our recent study exploring the role of *Notch* in HSC development (Souilhol et al., 2016b) failed to obtain any useful data using *in-utero*-induced gene ablation due to the highly resistant nature of the floxed *RbpJk* allele (our unpublished data).

In summary, our current study shows a crucial role for *Runx1* in HSC development in the AGM region prior to liver colonization, and emphasizes the value of *in vitro* models recapitulating developmental processes. Although studying biological processes *in vivo* is undeniably important, experiments involving induced gene modifications to analyze dynamic developmental processes *in utero* can incur major uncertainties. We believe that recapitulation of developmental processes *in vitro* using highly controlled conditions, supported by functional validation, will continue to play an important role in various areas of developmental biology.

EXPERIMENTAL PROCEDURES

Mice

All transgenic mice used to generate embryos and adult mice were on the C57BL/6 (CD45.2/2) background. $Rosa26Cre^{ERT2}$::$Runx1^{fl/fl}$ and $Rosa26Cre^{ERT2}$::sGFP::$Runx1^{fl/fl}$ mice were used to obtain $Rosa26Cre^{ERT2}$::sGFP::$Runx1^{fl/fl}$ conditional knockout and $Rosa26Cre^{ERT2}$::sGFP::$Runx1^{wt/fl}$ control embryos. The morning of discovery of the vaginal plug was designated as day 0.5. E11.5 embryos used had 41–45 somite pairs. C57BL/6 (*CD45.1/CD45.2*) animals were used as recipients for transplantations. $Rosa26Cre^{ERT2}$ were a gift from Lars Grotewold and Austin Smith, previously used in (Souilhol et al., 2016b); $Runx1^{fl/fl}$ mice and silent GFP (*sGFP*) mice were generated previously as described in (Putz et al., 2006) and (Gilchrist et al., 2003), respectively. All experiments with animals were performed under a Project License granted by the Home Office (UK), University of Edinburgh Ethical Review Committee, and conducted in accordance with local guidelines.

E11.5 AGM Explant Culture

AGM regions were dissected from E11.5 embryos and incubated for 2 hr at 37°C and 5% CO_2 in IMDM medium (Invitrogen)

Table 3. *Runx1* Genotype of E11.5 AGM Explant HSCs Assessed by PCR Analysis of Donor-Derived GFP+ Erythromyeloid Progenitors from Long-Term Engrafted Recipients

		Embryos with *Runx1* Recombined Alleles/Total Embryos (Recombination Range) HSC-Derived CFU-Cs (BM + Blood)			Total Colonies Analyzed
Experiment	Embryo Genotype	wt/Δ	fl/Δ	Δ/Δ	
iE9.5 -> E13.5 FL	*R26CreERT2::Runx1*$^{wt/fl}$	4/6 (11%–43%)			71
	R26CreERT2::Runx1$^{fl/fl}$		10/12 (14%–64%)	0/12 (NA)	127

Recombination range refers to proportion of recombined colonies.
NA, not applicable.

supplemented with 20% fetal calf serum (FCS) (HyClone, Fisher Scientific), L-glutamine (L-Gln), and penicillin/streptomycin (P/S). AGM regions were transferred individually onto 0.8 μm mixed cellulose MF membranes (AAWP02500, Millipore) for 5–7 days (37°C, 5% CO_2) and cultured at the liquid-gas interface with IMDM$^+$ medium consisting of 20% FCS, L-Gln, P/S IMDM, and growth factors (interleukin-3, SCF, and FLT3L, 100 ng/mL each; all from PeproTech). After 4 days of culture, explants were dissociated by enzymatic digestion (collagenase/dispase in PBS containing $CaCl_2$ and $MgCl_2$). Methylcellulose CFU-C and long-term repopulation assays were subsequently performed.

Hematopoietic Clonogenic Progenitor (CFU-C) and Colony Genotyping

Cell suspensions from either fresh or cultured embryonic tissues were plated into semi-solid Methocult M3434 medium (StemCell Technologies). After 7–12 days of culture, CFU-C colonies were scored and recombination in the *Runx1* locus analyzed by PCR. In brief, colonies were individually transferred into 50 μL of lysis buffer, incubated for 1 hr at 56°C followed by 5 min at 95°C. *Runx1*^{wt} (251 bp), *Runx1*^{fl} (325 bp), and *Runx1*^{Δ} (382 bp) products were amplified by simultaneously using the primers P5 (5′-TAGGGAGTGCTGCTTGCTCT-3′), P6 (5′- GCCGGGTGCAA. ATTAAGTC-3′), and P7 (5′-CTCTGGGAAACCAGGGAGTG-3′), under the following PCR conditions: 94°C 5 min; [94°C 30 s; 60°C 30 s; 72°C 1 min] × 35 cycles; 72°C 10 min.

Long-Term Hematopoietic Repopulation Assays

Cell suspensions from embryos at different stages were injected into irradiated adult recipients (*CD45.1/2*) either directly (E13.5 FL, 0.2 embryo equivalents per recipient mouse) or after explant culture (E11.5 AGM, 0.1 embryo equivalents per recipient mouse), along with 80,000 *CD45.1/1* bone marrow carrier cells. Recipients were irradiated by split dose (472 + 472 rad with 3-hr interval) of γ irradiation. Donor-derived chimerism was monitored in blood at 6 and 16 weeks after transplantation using FACScalibur (BD). Peripheral blood was collected by bleeding the lateral tail vein into 500 μL 5 mM EDTA/PBS, and erythrocytes were depleted using PharM Lyse (BD). Cells were stained with anti-CD16/32 (Fc-block, cat. no. 16-0161-86), CD45.1-APC (clone A20, cat. no. 17-0453-82), and anti-CD45.2-PE (clone 104, cat. no. 12-0454-83) monoclonal antibodies (eBioscience). Appropriate isotype controls were used. Dead cells were excluded using 7AAD (eBioscience). Mice demonstrating ≥5% donor-derived multilineage chimerism after 8 weeks were considered to be reconstituted.

Intraperitoneal Injections

Rosa26Cre^{ERT2}*::sGFP::Runx1*$^{fl/fl}$ and *Rosa26Cre*^{ERT2}*::sGFP::Runx1*$^{wt/fl}$ embryos were induced *in vivo* by intraperitoneal injection of 2 mg 4-OHT (Sigma) into *Rosa26Cre*^{ERT2}*::sGFP::Runx1*$^{wt/fl}$ x *Rosa26 Cre*^{ERT2}*::sGFP::Runx1*$^{fl/fl}$ pregnant females. 4-OHT was prepared in 100% ethanol, diluted 1:10 in corn oil. Embryos were allowed to develop *in utero* up to E11.5 or E13.5 before harvesting tissues for analysis by CFU-C, flow cytometry, and repopulation assays.

Testing Persistence of 4-OHT in Peripheral Blood of Adult Mice

C57BL/6 females were injected with 4-OHT as described above. Peripheral blood was collected by submandibular bleeding before 4-OHT injection (0 hr), 5, 20, 48, and 72 hr following injection. After centrifugation (400 × *g*/5 min), serum was collected and additionally centrifuged (400 × *g*/5 min) to remove remaining blood cells. Serum was frozen at −80°C and used at the same time in two independent sets of experiments. Total E10-11 AGM cells cultured for 24 hr in IMDM + 50% mouse serum were collected and analyzed by flow cytometry for GFP expression (dead cells were excluded by 7AAD). In some cases the cells were stained for CD45-PE (Pharmingen, cat. no. 553081) and VE-Cadherin-AlexaFluor-647 (eBioscience, cat. no. 51-1441-82; 138006).

SUPPLEMENTAL INFORMATION

Supplemental Information includes three figures and can be found with this article online at https://doi.org/10.1016/j.stemcr.2018.08.004.

AUTHOR CONTRIBUTIONS

J.S., A.B., S.R., S.G.-K., C.S., D.H., and S.Z. performed experiments. J.S. and A.M. designed the research. J.S. made figures and analyzed data. J.S. and A.M. wrote the paper. F.B. provided essential materials. A.M. provided overall supervision.

ACKNOWLEDGMENTS

The authors thank J. Verth and C. Manson for assistance with mouse maintenance and breeding; A. Dyer for irradiations. We thank Drs. Lars Grotewold and Austin Smith for the *RosaCreERT2*

mice. The authors thank Dr. A. Binagui-Casas for helpful comments. This work was supported by the Medical Research Council.

Received: June 7, 2018
Revised: August 2, 2018
Accepted: August 3, 2018
Published: August 30, 2018

REFERENCES

Bertrand, J.Y., Chi, N.C., Santoso, B., Teng, S., Stainier, D.Y., and Traver, D. (2010). Haematopoietic stem cells derive directly from aortic endothelium during development. Nature *464*, 108–111.

Boisset, J.C., Clapes, T., Klaus, A., Papazian, N., Onderwater, J., Mommaas-Kienhuis, M., Cupedo, T., and Robin, C. (2015). Progressive maturation toward hematopoietic stem cells in the mouse embryo aorta. Blood *125*, 465–469.

Cai, Z., de Bruijn, M., Ma, X., Dortland, B., Luteijn, T., Downing, R.J., and Dzierzak, E. (2000). Haploinsufficiency of AML1 affects the temporal and spatial generation of hematopoietic stem cells in the mouse embryo. Immunity *13*, 423–431.

Cai, X., Gaudet, J.J., Mangan, J.K., Chen, M.J., De Obaldia, M.E., Oo, Z., Ernst, P., and Speck, N.A. (2011). Runx1 loss minimally impacts long-term hematopoietic stem cells. PLoS One *6*, e28430.

Chen, M.J., Yokomizo, T., Zeigler, B.M., Dzierzak, E., and Speck, N.A. (2009). Runx1 is required for the endothelial to haematopoietic cell transition but not thereafter. Nature *457*, 887–891.

Chen, M.J., Li, Y., De Obaldia, M.E., Yang, Q., Yzaguirre, A.D., Yamada-Inagawa, T., Vink, C.S., Bhandoola, A., Dzierzak, E., and Speck, N.A. (2011). Erythroid/myeloid progenitors and hematopoietic stem cells originate from distinct populations of endothelial cells. Cell Stem Cell *9*, 541–552.

Ciau-Uitz, A., Patient, R., and Medvinsky, A. (2016). Ontogeny of the haematopoietic system. In Encyclopedia of Immunobiology, vol. 1, M.J.H. Ratcliffe, ed. *(Academic Press), pp. 1–14*.

Clements, W.K., Kim, A.D., Ong, K.G., Moore, J.C., Lawson, N.D., and Traver, D. (2011). A somitic Wnt16/Notch pathway specifies haematopoietic stem cells. Nature *474*, 220–224.

de Bruijn, M.F., Ma, X., Robin, C., Ottersbach, K., Sanchez, M.J., and Dzierzak, E. (2002). Hematopoietic stem cells localize to the endothelial cell layer in the midgestation mouse aorta. Immunity *16*, 673–683.

Eliades, A., Wareing, S., Marinopoulou, E., Fadlullah, M.Z.H., Patel, R., Grabarek, J.B., Plusa, B., Lacaud, G., and Kouskoff, V. (2016). The hemogenic competence of endothelial progenitors is restricted by Runx1 silencing during embryonic development. Cell Rep. *15*, 2185–2199.

Ferkowicz, M.J., Starr, M., Xie, X., Li, W., Johnson, S.A., Shelley, W.C., Morrison, P.R., and Yoder, M.C. (2003). CD41 expression defines the onset of primitive and definitive hematopoiesis in the murine embryo. Development *130*, 4393–4403.

Fitch, S.R., Kimber, G.M., Wilson, N.K., Parker, A., Mirshekar-Syahkal, B., Gottgens, B., Medvinsky, A., Dzierzak, E., and Ottersbach, K. (2012). Signaling from the sympathetic nervous system regulates hematopoietic stem cell emergence during embryogenesis. Cell Stem Cell *11*, 554–566.

Gama-Norton, L., Ferrando, E., Ruiz-Herguido, C., Liu, Z., Guiu, J., Islam, A.B., Lee, S.U., Yan, M., Guidos, C.J., López-Bigas, N., et al. (2015). Notch signal strength controls cell fate in the haemogenic endothelium. Nat. Commun. *6*, 8510.

Gilchrist, D.S., Ure, J., Hook, L., and Medvinsky, A. (2003). Labeling of hematopoietic stem and progenitor cells in novel activatable EGFP reporter mice. Genesis *36*, 168–176.

Ivanovs, A., Rybtsov, S., Anderson, R.A., Turner, M.L., and Medvinsky, A. (2014). Identification of the niche and phenotype of the first human hematopoietic stem cells. Stem Cell Rep. *2*, 449–456.

Kissa, K., and Herbomel, P. (2010). Blood stem cells emerge from aortic endothelium by a novel type of cell transition. Nature *464*, 112–115.

Lee, Y., Manegold, J.E., Kim, A.D., Pouget, C., Stachura, D.L., Clements, W.K., and Traver, D. (2014). FGF signalling specifies haematopoietic stem cells through its regulation of somitic Notch signalling. Nat. Commun. *5*, 5583.

Liakhovitskaia, A., Rybtsov, S., Smith, T., Batsivari, A., Rybtsova, N., Rode, C., de Bruijn, M., Buchholz, F., Gordon-Keylock, S., Zhao, S., et al. (2014). Runx1 is required for progression of CD41+ embryonic precursors into HSCs but not prior to this. Development *141*, 3319–3323.

Lie-A-Ling, M., Marinopoulou, E., Lilly, A.J., Challinor, M., Patel, R., Lancrin, C., Kouskoff, V., and Lacaud, G. (2018). Regulation of RUNX1 dosage is crucial for efficient blood formation from hemogenic endothelium. Development *145*. https://doi.org/10.1242/dev.149419.

Lizama, C.O., Hawkins, J.S., Schmitt, C.E., Bos, F.L., Zape, J.P., Cautivo, K.M., Borges Pinto, H., Rhyner, A.M., Yu, H., Donohoe, M.E., et al. (2015). Repression of arterial genes in hemogenic endothelium is sufficient for haematopoietic fate acquisition. Nat. Commun. *6*, 7739.

McGrath, K.E., Frame, J.M., Fegan, K.H., Bowen, J.R., Conway, S.J., Catherman, S.C., Kingsley, P.D., Koniski, A.D., and Palis, J. (2015). Distinct sources of hematopoietic progenitors emerge before HSCs and provide functional blood cells in the mammalian embryo. Cell Rep. *11*, 1892–1904.

Medvinsky, A., and Dzierzak, E. (1996). Definitive hematopoiesis is autonomously initiated by the AGM region. Cell *86*, 897–906.

Medvinsky, A.L., Samoylina, N.L., Muller, A.M., and Dzierzak, E.A. (1993). An early pre-liver intraembryonic source of CFU-S in the developing mouse. Nature *364*, 64–67.

Muller, A.M., Medvinsky, A., Strouboulis, J., Grosveld, F., and Dzierzak, E. (1994). Development of hematopoietic stem cell activity in the mouse embryo. Immunity *1*, 291–301.

North, T., Gu, T.L., Stacy, T., Wang, Q., Howard, L., Binder, M., Marin-Padilla, M., and Speck, N.A. (1999). Cbfa2 is required for the formation of intra-aortic hematopoietic clusters. Development *126*, 2563–2575.

North, T.E., de Bruijn, M.F., Stacy, T., Talebian, L., Lind, E., Robin, C., Binder, M., Dzierzak, E., and Speck, N.A. (2002). Runx1 expression marks long-term repopulating hematopoietic stem cells in the midgestation mouse embryo. Immunity *16*, 661–672.

Okuda, T., van Deursen, J., Hiebert, S.W., Grosveld, G., and Downing, J.R. (1996). AML1, the target of multiple chromosomal

translocations in human leukemia, is essential for normal fetal liver hematopoiesis. Cell *84*, 321–330.

Palis, J., Robertson, S., Kennedy, M., Wall, C., and Keller, G. (1999). Development of erythroid and myeloid progenitors in the yolk sac and embryo proper of the mouse. Development *126*, 5073–5084.

Peeters, M., Ottersbach, K., Bollerot, K., Orelio, C., de Bruijn, M., Wijgerde, M., and Dzierzak, E. (2009). Ventral embryonic tissues and Hedgehog proteins induce early AGM hematopoietic stem cell development. Development *136*, 2613–2621.

Pouget, C., Peterkin, T., Simoes, F.C., Lee, Y., Traver, D., and Patient, R. (2014). FGF signalling restricts haematopoietic stem cell specification via modulation of the BMP pathway. Nat. Commun. *5*, 5588.

Putz, G., Rosner, A., Nuesslein, I., Schmitz, N., and Buchholz, F. (2006). AML1 deletion in adult mice causes splenomegaly and lymphomas. Oncogene *25*, 929–939.

Richard, C., Drevon, C., Canto, P.Y., Villain, G., Bollérot, K., Lempereur, A., Teillet, M.A., Vincent, C., Rosselló Castillo, C., Torres, M., et al. (2013). Endothelio-mesenchymal interaction controls runx1 expression and modulates the notch pathway to initiate aortic hematopoiesis. Dev. Cell *24*, 600–611.

Robin, C., Ottersbach, K., Durand, C., Peeters, M., Vanes, L., Tybulewicz, V., and Dzierzak, E. (2006). An unexpected role for IL-3 in the embryonic development of hematopoietic stem cells. Dev. Cell *11*, 171–180.

Rybtsov, S., Sobiesiak, M., Taoudi, S., Souilhol, C., Senserrich, J., Liakhovitskaia, A., Ivanovs, A., Frampton, J., Zhao, S., and Medvinsky, A. (2011). Hierarchical organization and early hematopoietic specification of the developing HSC lineage in the AGM region. J. Exp. Med. *208*, 1305–1315.

Rybtsov, S., Batsivari, A., Bilotkach, K., Paruzina, D., Senserrich, J., Nerushev, O., and Medvinsky, A. (2014). Tracing the origin of the HSC hierarchy reveals an SCF-dependent, IL-3-independent CD43(–) embryonic precursor. Stem Cell Rep. *3*, 489–501.

Rybtsov, S., Ivanovs, A., Zhao, S., and Medvinsky, A. (2016). Concealed expansion of immature precursors underpins acute burst of adult HSC activity in foetal liver. Development *143*, 1284–1289.

Souilhol, C., Gonneau, C., Lendinez, J.G., Batsivari, A., Rybtsov, S., Wilson, H., Morgado-Palacin, L., Hills, D., Taoudi, S., Antonchuk, J., et al. (2016a). Inductive interactions mediated by interplay of asymmetric signalling underlie development of adult haematopoietic stem cells. Nat. Commun. *7*, 10784.

Souilhol, C., Lendinez, J.G., Rybtsov, S., Murphy, F., Wilson, H., Hills, D., Batsivari, A., Binagui-Casas, A., McGarvey, A.C., MacDonald, H.R., et al. (2016b). Developing HSCs become notch independent by the end of maturation in the AGM region. Blood *128*, 1567–1577.

Tanaka, Y., Hayashi, M., Kubota, Y., Nagai, H., Sheng, G., Nishikawa, S., and Samokhvalov, I.M. (2012). Early ontogenic origin of the hematopoietic stem cell lineage. Proc. Natl. Acad. Sci. USA *109*, 4515–4520.

Taoudi, S., and Medvinsky, A. (2007). Functional identification of the hematopoietic stem cell niche in the ventral domain of the embryonic dorsal aorta. Proc. Natl. Acad. Sci. USA *104*, 9399–9403.

Taoudi, S., Gonneau, C., Moore, K., Sheridan, J.M., Blackburn, C.C., Taylor, E., and Medvinsky, A. (2008). Extensive hematopoietic stem cell generation in the AGM region via maturation of VE-cadherin+CD45+ pre-definitive HSCs. Cell Stem Cell *3*, 99–108.

Tober, J., Yzaguirre, A.D., Piwarzyk, E., and Speck, N.A. (2013). Distinct temporal requirements for Runx1 in hematopoietic progenitors and stem cells. Development *140*, 3765–3776.

Tober, J., Maijenburg, M.M.W., Li, Y., Gao, L., Hadland, B.K., Gao, P., Minoura, K., Bernstein, I.D., Tan, K., and Speck, N.A. (2018). Maturation of hematopoietic stem cells from prehematopoietic stem cells is accompanied by up-regulation of PD-L1. J. Exp. Med. *215*, 645–659.

Yzaguirre, A.D., Howell, E.D., Li, Y., Liu, Z., and Speck, N.A. (2018). Runx1 is sufficient for blood cell formation from non-hemogenic endothelial cells in vivo only during early embryogenesis. Development *145*. https://doi.org/10.1242/dev.158162.

Zhou, F., Li, X., Wang, W., Zhu, P., Zhou, J., He, W., Ding, M., Xiong, F., Zheng, X., Li, Z., et al. (2016). Tracing haematopoietic stem cell formation at single-cell resolution. Nature *533*, 487–492.